

# Titania from nanoclusters to nanowires and nanoforks

G. Wang<sup>1,a</sup> and G. Li<sup>2</sup>

<sup>1</sup> National Laboratory of Solid State Microstructures, Nanjing University, Nanjing 210093, P.R. China

<sup>2</sup> Center for Advanced Studies of Science and Technology, Nanjing 210093, P.R. China

Received 10 September 2002

Published online 3 July 2003 – © EDP Sciences, Società Italiana di Fisica, Springer-Verlag 2003

**Abstract.** A novel method – inverse microemulsion has been developed not only for synthesizing low cost TiO<sub>2</sub> nanoclusters but also for the first time preparing titania nanowires and nanoforks with rutile structure of single crystal. With two microemulsion systems, spherical TiO<sub>2</sub> nanoclusters of 5 nm in average diameter are produced. These nanoclusters are amorphous and turned into anatase at an annealing temperature lower than 750 °C, and changed into rutile when annealed at higher temperature. When three microemulsions with TiCl<sub>4</sub>, ammonia and NaCl as aqueous phase, are used, the precursor powder containing Ti(OH)<sub>4</sub>/NaCl with molar ratio of 1000 are annealed at 750 °C and then TiO<sub>2</sub> rutile nanowires with 22 nm in thickness and 4 μm in length are formed. At the same time two kinds of nanoforks with defined boundary structures are constructed: one is a bent wire composed of two straight whiskers related by twinning on a (101) plane with the angle of 114° between the two legs, and the other by twinning on a (301) planes with the angle of 55° between the legs. Screw dislocations and a periodic structure are found in (301) twin boundary, while edge dislocations are observed in (101) twin boundaries. The experiments demonstrate that the titania rutile nanowires are formed through solid state phase transformation and sodium chloride play an important role in the process.

**PACS.** 61.46.+w Nanoscale materials: clusters, nanoparticles, nanotubes, and nanocrystals

## 1 Introduction

Titania exhibits some unique dielectric and chemical properties that can be utilized in various technological applications such as photocatalysts [1], ceramic membranes [2], humidity sensors [3,4] and gas sensors [5]. However, it is frequently used in the form of nanoparticles prepared by gas condensation [6] and sol-gel methods [7,8]. Here we report a method using several microemulsion systems [9] developed not only for synthesizing low cost TiO<sub>2</sub> nanoclusters but also for the first time preparing titania nanowires with rutile structure of single crystal [10] and discuss a possible growth mechanism of titania rutile nanowires.

## 2 Experimental

An inverse microemulsion system, which consists of an oil phase, a surfactant phase and an aqueous phase, is a thermodynamically stable isotropic dispersion of the aqueous phase in the continuous oil phase [11]. To prepare inverse microemulsions, a cyclohexane (analytical reagent) was used as the oil phase and a mixture of poly(oxyethylene)<sub>5</sub> nonyle phenol ether (NP5, chemical purity) and poly(oxyethylene)<sub>9</sub> nonyle phenol ether

(NP9, chemical purity) with weight ratio 1:1 as the non-ionic surfactant (NP5-NP9). Two microemulsion systems were prepared, containing a 0.5 M titanium tetrachloride (TiCl<sub>4</sub>) aqueous solution and a 2.0 M ammonia as the aqueous phase, respectively. The ammonia was analytical reagent grade and the TiCl<sub>4</sub> was of chemical purity. The distilled water was used and the aqueous TiCl<sub>4</sub> solution was prepared by the method proposed by Park *et al.* [12]. The oil phase, surfactant and aqueous phase in an appropriate proportion were mixed in a beaker at 13 °C in a water bath to form the microemulsion. Appropriate amounts of microemulsion I containing 0.5 M TiCl<sub>4</sub> aqueous solution and microemulsion II containing 2.0 M ammonia were mixed together, leading to the formation of insoluble titania particles. The mixed microemulsions were then poured into acetone to precipitate TiO<sub>2</sub> nanoparticles, which were then washed by the use of a centrifuge and acetone, followed by vacuum drying for two hours. The virgin product is a white powder of amorphous TiO<sub>2</sub> nanoclusters with average diameter of 5 nm, and transformed into the crystalline anatase by heating from 200 to 750 °C, and then into rutile at temperature higher than 750 °C. The transition point from amorphous to anatase is 390 °C while the transition point from anatase to rutile is 750 °C.

For the nanowires, three microemulsion systems were prepared, containing a 0.5 M titanium tetrachloride (TiCl<sub>4</sub>) aqueous solution, 2.0 M ammonia solution

<sup>a</sup> e-mail: ghwang@nju.edu.cn

**Table 1.** Compositions of the microemulsions used in preparing rutile TiO<sub>2</sub> nanowires.

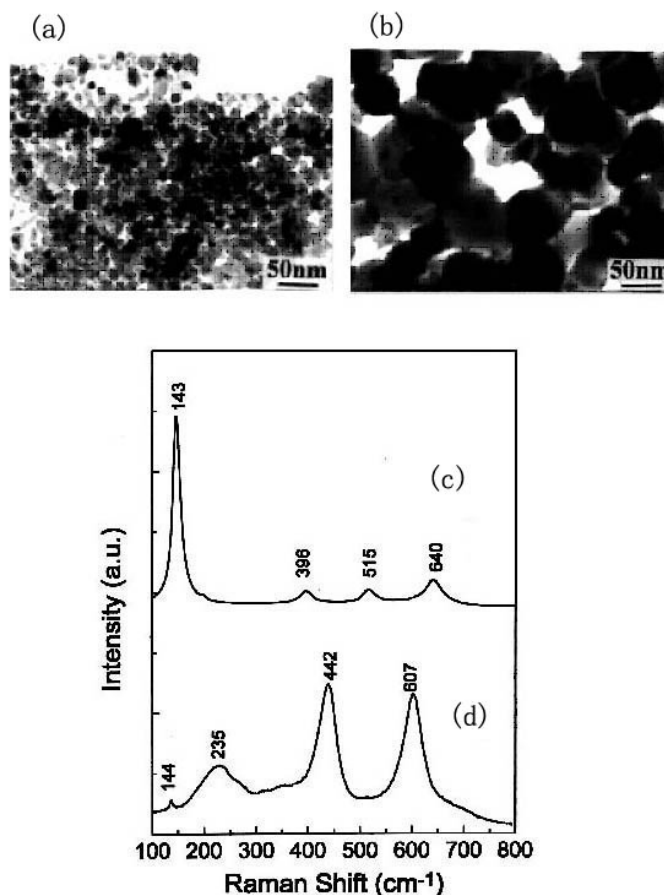
	microemulsion I	microemulsion II	microemulsion III
aqueous phase (vol.%)	0.5 M TiCl <sub>4</sub> (2%)	2.0 M ammonia (2%)	2.0 M NaCl (20%)
surfactant (vol.%)	NP5-NP9 (33%)	NP5-NP9 (33%)	NP5-NP9 (28%)
oil phase (vol.%)	cyclohexane (65%)	cyclohexane (65%)	cyclohexane (65%)

and a 2.0 M NaCl aqueous solution as the aqueous phase, respectively. NaCl was also of analytical grade. The rest procedure of the experiments is almost the same as that for preparing the TiO<sub>2</sub> nanoclusters except adding certain amount of NaCl and changing compositions in the microemulsions. The compositions of the microemulsions used are listed in Table 1. All characterizations were carried out at room temperature.

### 3 Nanoclusters and nanowires of titania

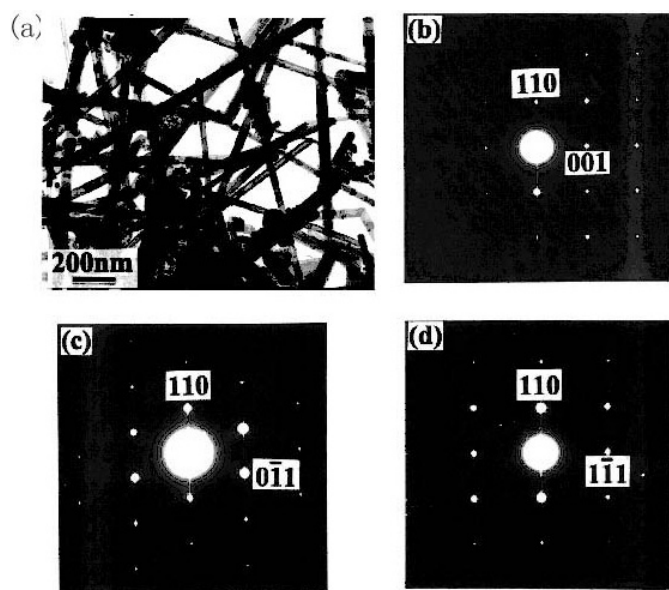
Figures 1a and 1b shows TEM images of the virgin samples: (Fig. 1a) calcined for 2 hours at 500 °C and (Fig. 1b) calcined for 2 hours at temperature of 800 °C. Figures 1c and 1d give their corresponding Raman spectra. The clusters have the anatase structure with average size of 10 nm in the former case while the particles grow up to 60 nm in diameter with rutile structure in the latter, but no wire-like morphology is observed in such process.

Figure 2 shows the morphology and crystal structure of the product obtained by annealing the precursor powder with the molar ratio of sodium to titanium ( $\gamma = 400$ ) at 750 °C for 2 hours. TEM image in Figure 2a demonstrates that the sample consists of straight, solid wires with diameters ranging from 10 to 50 nm and lengths of  $>2 \mu\text{m}$ . The crystal structure of these nanowires is determined by a set of selected area diffraction patterns (SASPs, Figs. 2b–2d) obtained from a single nanowire of them from different orientations of [110], [111] and [112], identifying that the nanowires have rutile structure with the wire axis parallel to [001] direction. High resolution TEM(HREM) images recorded on individual nanowires (Fig. 3) proved further insight into their structure. A low magnification HREM image (Fig. 3A) shows that the nanowire is a perfect crystal without planar defects. The side surfaces are (110) planes and the tip of the nanowires is terminated by {111} planes, indicating the (111) planes are most favorable for growth of the nanowires, which is sketched in Figure 3B, and further supported by XRD studies [13]. Figure 3C shows high resolution images of electron microscope of such nanowire demonstrate that the side surface (110) of the nanowire is smooth at atomic scale and no obvious contrast difference can be seen between the surface layer and the inner part of the wire, indicating the nanowires with square cross sections and four {110} planes for side surfaces. Figure 3D is the HREM image of the nanowire tip with (111) planes as its preferential. We have systematically investigated influences of various experimental conditions and found that the quality of the nanowires depends on the annealing temperature and the relative amount of Ti(OH)<sub>4</sub> particles as well



**Fig. 1.** (a) and (b) TEM (JEOL-200CX) images of the samples (titania nanoclusters) prepared by two microemulsion systems containing a 0.5 M titanium tetrachloride (TiCl<sub>4</sub>) solution and a 2.0 M ammonia as the aqueous phase, respectively: (a) calcined for 2 hours at 500 °C, (b) calcined for 2 hours at 800 °C, (c) Raman spectra of the corresponding samples: up-curve for (a), and (d) down-curve for (b), indicating the former with anatase structure and the latter with rutile structure.

as homogeneity of titanium hydroxide particles dispersed in sodium chloride particles in the precursor powder. At the annealing temperature of 730 °C, the product mainly consists of small spherical particles with anatase structure, and only a few very thin rutile nanowires have been observed, and then number of the nanowires gradually increases as the temperature goes higher because more anatase particles are transformed into rutile phase. However, when the temperature goes higher than 750 °C the nanowires become thicker and shorter than those obtained at 750 °C, though their structure is rutile. The thickness of most wires reaches several hundreds of nanometers when



**Fig. 2.** (a) TEM (JEOL-200CX) bright field image of the resultant of the powder with  $\gamma = 400$  prepared by three microemulsion systems containing a 0.5 M titanium tetrachloride ( $\text{TiCl}_4$ ) solution, 2.0 M ammonia solution and a 2.0 M aqueous solution as the aqueous phase, respectively, annealed at  $750^\circ\text{C}$  for 2 hours, showing that most products are nanowires and small amount of particles are sodium titanates. (b–d) Selected area diffraction patterns (SADP) from the same area of an individual nanowire from different directions: (b) SADP in  $[110]$  zone, (c) SADP in  $[111]$  zone obtained by tilting the same nanowire corresponding to (b)  $25^\circ$  along the  $[110]$  axis, (d) SADP in  $[112]$  zone obtained by further tilting the same nanowire  $18^\circ$  along the  $[110]$  axis, indicating that the nanowires are rutile  $\text{TiO}_2$  and their axis is  $[001]$ . The elongation of the diffraction spots is due to relaxation of the surface layer of the nanowire.

**Table 2.** Amount of microemulsions ( $\mu\text{E}$ ) used for the preparation of precursor powders and average sizes of the rutile nanowires.

$\mu\text{E}$ I (ml)	$\mu\text{E}$ II (ml)	$\mu\text{E}$ III (ml)	$\gamma^*$	average sizes of nanowires ( $\mu\text{m} \times \text{nm}$ )
4	4	12	100	$2 \times 75$
2	2	24	400	$2 \times 30$
1	1	30	1000	$4 \times 22$

\*  $\gamma$  is the molar ratio of sodium to titanium in precursor powder which can be obtained by controlling the relative amount of  $\text{TiCl}_4$ , ammonia and  $\text{NaCl}$  in the microemulsion.

the annealing temperature increases up to  $800^\circ\text{C}$ . The density of  $\text{Ti}(\text{OH})_4$  in the precursor powder also affects the formation of rutile nanowires. Table 2 summarizes the average sizes of the nanowires transformed from precursor powders of different  $\gamma$  values. In general, the greater the  $\gamma$  value, the thinner and longer the nanowires. When  $\gamma$  is equal to 1000, the nanowires with average thickness of 20 nm and length of  $4 \mu\text{m}$  are obtained but a considerable amount of precursor particles directly transform into spherical rutile particles. Therefore, certain amount

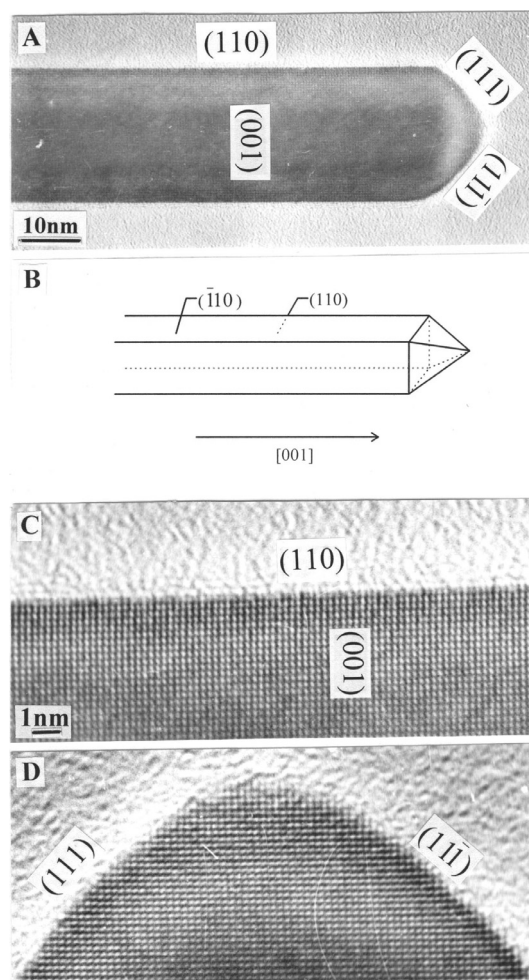


**Fig. 3.** HREM (JOEL-2000EX) images of the nanowires along the  $[110]$  direction. (A) low magnification image showing the single crystal nanowire with the side surfaces of  $(110)$  planes and the tip surface of  $\{111\}$  planes, (B) sketch of a such nanowire, (C) profile image of a  $(110)$  side surface smooth at atomic scale, (D) profile image of surfaces of the nanowire tip.

of  $\text{NaCl}$  is one of key points in the formation of rutile nanowires.

Figures 4A–4C show the TEM images of the products of the precursor powder with  $\gamma = 400$  annealed at  $750^\circ\text{C}$  for 5, 10 and 30 min respectively. In Figure 4A, the white product consists of two kinds of small particles: small irregular ones are identified as anatase phase and the larger ones with rectangular shapes are rutile. With 10 min annealing only a few nanowires are observed (Fig. 4B). After 30 min annealing more nanowires are formed at expense of anatase particles (Fig. 4C) but the thickness of the wires do not change much. Figure 4D shows the magnified image of one of the wires selected from Figure 4C in which some of the nanoparticles with anatase structure are surrounded at the top of the wire tip. Almost all the precursor particles are transformed into rutile nanowires after annealing for 2 hours (see Fig. 2A), indicating that solid state phase transformation exists in the formation of rutile nanowires during annealing.

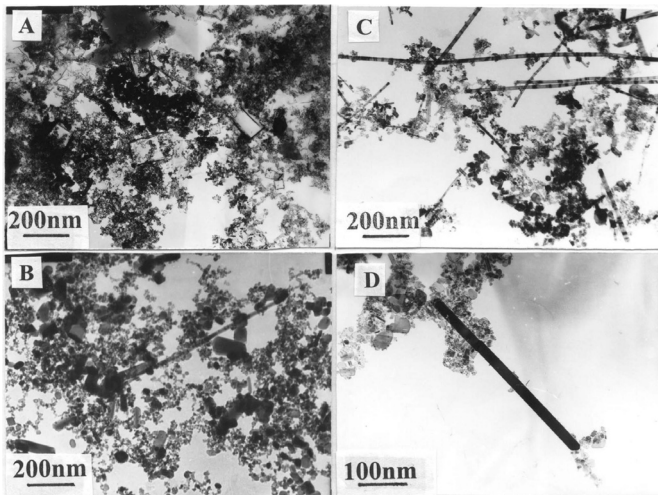
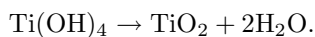


**Fig. 4.** TEM images of the products with same compositions ( $\gamma = 400$ ) as those in Figure 2 but annealed at 750 °C for different times: (A) 5 min, showing large amount of small irregular particles with anatase structure and a few of rutile rectangular grains; (B) 10 min, exhibiting very few of thin and longer nanowires; and (C) 30 min, showing certain amount of the nanowires; (D) the magnified image of one of the wires selected from (C) in which some of the nanoparticles with anatase structure are surrounded at the top of the wire tip.

For VLS [14] and SLS [15] approaches, whisker growth requires a fluid phase (vapor in VLS and solution in SLS) in which elements of the crystal phase can easily move for a long distance. In our case, the  $\text{Ti}(\text{OH})_4$  particles are homogeneously dispersed in the NaCl particles without aggregation or agglomeration. Here, at first NaCl plays roles of separating the  $\text{Ti}(\text{OH})_4$  particles and promoting their diffusion. In order to get an idea of growth mechanism of the nanowires we have investigated the behavior of the mixed powder before annealing by TEM and found that the  $\text{Ti}(\text{OH})_4$  particles move quickly under irradiation of sufficiently intensive electron beam on the one hand, and on the other we have looked steadily at one of wires in the sample with  $\gamma = 400$  annealed at 750 °C only for 30 min by TEM (shown in Fig. 4D) and found that small titania particles with diameter of  $\sim 4$  nm moved slowly both from nearby and the side surfaces towards the tip of the rutile whisker and finally transformed into the rutile structure at the tip under the irradiation of the intensive electron beam. The process is schematically illustrated in Figure 5. Therefore, the growth sequences of the titania rutile nanowires during annealing are suggested as follows: (1) when the powder containing NaCl and  $\text{Ti}(\text{OH})_4$  is heated up to 750 °C, certain amount of rectangular rutile grains (or short whiskers) are formed as nuclei and at same time the titanium hydroxide particles are decomposed into anatase  $\text{TiO}_2$  particles:



(2) Anatase particles diffuse and move to the short whisker tips and then transform into the rutile structure on the tip of the whisker due to mobility of atoms and bond

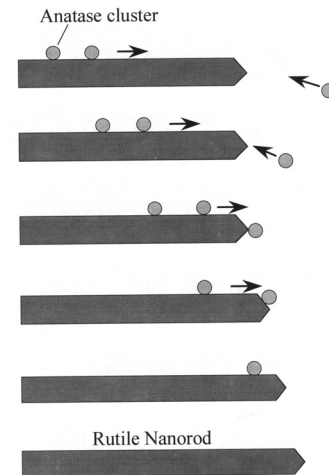


**Fig. 5.** Schematic illustration of growth sequence of a rutile nanowire by solid state phase transformation.

breakage [16], finally making rutile nanowires through solid state transformation [17]. From these discussions it seems that NaCl particles do not play direct role in the above process. However, we can not obtain the titania nanowires but only nanoclusters (shown in Fig. 1) without NaCl. In order to study the effect of NaCl further we have mixed  $\text{Ti}(\text{OH})_4$  directly with sodium chloride powder rather than in the form of microemulsion for annealing, and also observed existence of the  $\text{TiO}_2$  nanowires after annealing although the nanowires formed in such case are not uniform and the productivity is low. This implies that sodium chloride particles play roles of not only separating and promoting diffusion of  $\text{Ti}(\text{OH})_4$  particles mentioned above but also promoting formation of the rectangular rutile nanograins as well as transformation from anatase to rutile during annealing. However, at present we do not know the exact role of chemical reactions of NaCl with  $\text{TiO}_2$  that lead to the formation of sodium titanates during the nanowire growth. Recently, Gesehues has found  $\text{Al}^{+3}$ -doped  $\text{TiO}_2$  affecting the phase transformation and growth of titania [18]. It is possible that  $\text{Na}^+$  may contribute to the formation of rutile nanowires in a similar way.

#### 4 Nanoforks and their interfaces

In the above process the products mostly consist of straight, rod-like whiskers. At the same time a certain amount of  $\text{TiO}_2$  twined crystals like nanoforks is formed, shown in Figure 6. Two kinds of twined whiskers are formed, and each with two legs constructing an angle of 55° and 114° respectively. The legs have a common [010] direction. However, in Figure 6a the two legs are related by twinning on the (301) plane with each other, and its selected area diffraction pattern (SADP) is taken in Figure 8b. From Figures 6c and 6d the two legs of the fork are related by twinning on (101) plane and the axis of each leg is along the [001] direction.

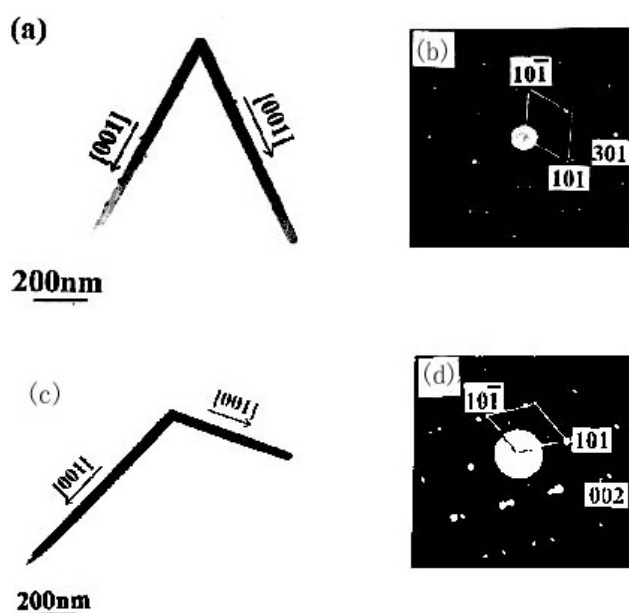


**Fig. 6.** (a) TEM image of a  $\text{TiO}_2$  nanofork with  $(301)$  interface, and (b) selected area diffraction pattern of the twined boundary between the two legs. (c) TEM image of a nanofork and (d) the SADP of its  $(101)$  twined boundary.

Microstructures of these twined boundaries have been studied by high resolution electron microscope (HREM). Figure 7a shows low magnification HREM image of  $(301)$  twined boundary when electron beam is parallel to  $[010]$  direction. A dislocation can be seen and the dislocation line parallel to the electron beam, *i.e.*, along  $[010]$  direction. Figure 7b is the magnification image of the area including the dislocation around the point B, and this dislocation is screw dislocation because Burgers vector is zero in the  $(010)$  plane ( $\mathbf{b} = [010]$ ). Figure 7c is the magnification image of the area at C indicated in Figure 7a, and at the twined interface a periodic structure appears with 6 distances between lattice plane  $(101)$ , quite different from the interfacial structure in the equilibrium condition [19]. Figure 8a is a HREM image of  $(101)$  twined interface along  $[010]$  direction at low magnification. There is a dislocation at the C point. Figure 8b is a magnified image of B point in (a), the atom arrangement is the same as the equilibrium structure. Figure 8c gives a magnified image of the dislocation region in Figure 8a. The dislocation is embedded in the interior of the twined whisker and fringes are parallel to the twined interface. An extra half atomic plane appears, indicating that the Burger vector of this dislocation includes the component of  $\frac{1}{2}[10\bar{1}]$ . Several other types of rutile  $\text{TiO}_2$  twined nanostructures are observed, such as a straight whisker with a branch related by twinning on a  $(301)$  plane, a nanowire with three legs, among which the two adjacent legs with an angle of  $55^\circ$  while the middle leg twined with its two neighbors  $\pm$  different  $\{301\}$  planes [20], etc. In fact a variety of morphologies of  $\text{TiO}_2$  twined nanowires have been found, however, only two kinds of twins,  $(101)$  and  $(301)$  twins exist, implying that the twin can form on any one

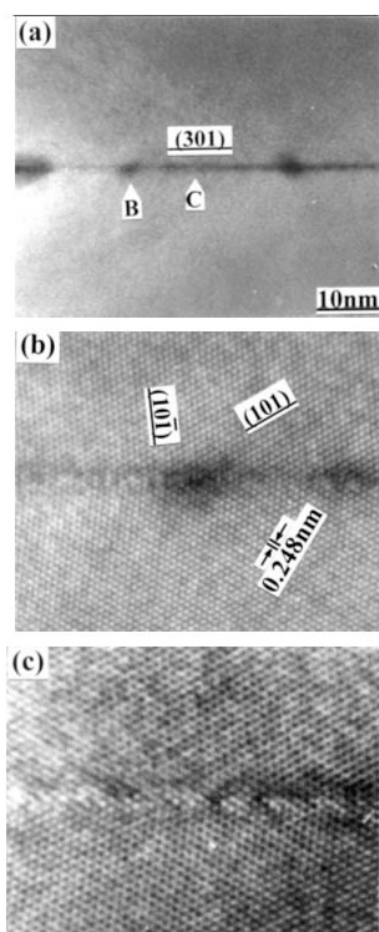


**Fig. 7.** HREM images of  $(301)$  twined boundary: (a) low magnification; (b) amplified image of B region in (a); (c) amplified image of C region in (a).

of the  $\{101\}$  or  $\{301\}$  planes. Similar situation also occurs in  $\text{SnO}_2$ , which has an isomorphous crystal structure with rutile form  $\text{TiO}_2$  [21].

## 5 Conclusions

We have developed the method using microemulsion systems not only synthesizing low cost  $\text{TiO}_2$  nanoclusters but also preparing titania nanowires with rutile structure free of defect through solid state phase transformation. Two types of nanoforks with defined boundary structures are constructed: one is a bent wire composed of two straight whiskers related by twinning on a  $(101)$  plane with the angle of  $114^\circ$  between the two legs, and the other by twinning on a  $(301)$  planes with the angle of  $55^\circ$  between the legs.

Titania surfaces play an important role in heterogeneous catalysis, photo-catalysis, gas-sensing and electrode-electrolyte interactions. The rutile  $(110)$  surface has been used as an ideal, thermodynamically stable surface in the study of semiconductor-gas interaction [22]. Titania used in these fields usually consists of particles with several crystal planes of different indices [23]. The  $\text{TiO}_2$  nanowires prepared by our present method have

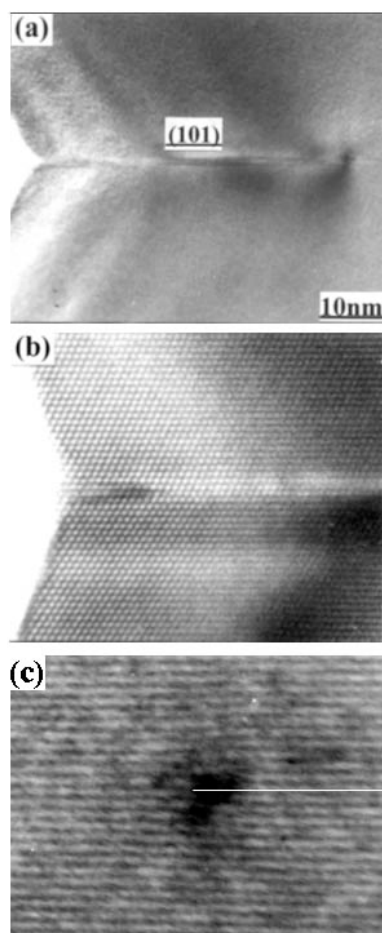


**Fig. 8.** HREM images of (101) twined boundary: (a) low magnification; (b) amplified image; (c) dislocation image at the interface.

more than 99% of its surfaces consisting of  $\{110\}$  planes. Furthermore, these nanowires are very easy to be curved or bent without breaking, and radius of curvature of the bent nanowires is as small as 500 nm. No grain boundary is found and density of dislocations is estimated to be  $\sim 7 \times 10^{11} \text{ cm}^{-2}$ , three or four order higher than that for the bulk titania, demonstrating that such nanowires are very soft and have novel mechanical property. Therefore, the materials composed of such nanowires can not only be employed as a prototype in the study of surface-related properties, and made as nano-sensors with very high sensitivity, but also can be used to weave a network and fabricate ceramic membranes with high mechanical strength and high temperature stability.

This work is supported by National Natural Science Foundation of China (No. 29890210; 10074024).

## References

1. G. Dagan, M. Tomkiewics, *J. Phys. Chem.* **97**, 12651 (1993)
2. Q. Xu, M.A. Anderson, *J. Am. Ceram. Soc.* **77**, 1939 (1994)
3. Y.C. Yeh, T.T. Tseng, D.A. Chang, *J. Am. Ceram. Soc.* **73**, 1992 (1990)
4. A.M. Katayama, H. Hasegawa, T. Noda, T. Akiba, H. Yanagida, *Sensors Actuators B* **2**, 143 (1992)
5. A.M. Azad, L.B. Youndman, S.A. Akbar, *J. Am Ceram. Soc.* **77**, 481 (1994)
6. R.W. Siegel, S. Ramasamy, H. Hahn, Z. Li, T. Lu, R. Gronsky, *J. Mater. Res.* **3**, 1367 (1988)
7. B.A. Morales, O. Novaro, T. Lopes, E. Sanches, R. Gomes, *J. Mater. Res.* **10**, 2788 (1995)
8. B.E. Yokdas, *J. Mater. Sci.* **21**, 1087 (1986)
9. G.L. Li, G.H. Wang, Chinese Patent No. 98111329.x, 1998
10. G.L. Li, G.H. Wang, J.M. Hong, *J. Mater. Res.* **14**(8), 3346 (1999)
11. J. Wang, L.S. Ee, S.C. Ng, C.H. Chew, L.M. Gan, *Mater. Lett.* **30**, 119 (1997)
12. H.K. Park, D.K. Kim, C.H. Kim, *J. Am. Ceram. Soc.* **80**, 743 (1997)
13. The shape and structure of the nanowires are further supported by XRD studies from a film prepared by depositing an alcohol dispersion containing such nanowires onto an amorphous silica substrate, followed by drying in air. Only the (110) and (220) peaks are observed while normally very strong peaks (101) and (211) in the rutile  $\text{TiO}_2$  disappear. Therefore, one of  $\{110\}$  planes of most nanowires in the film are parallel or nearly parallel to the surface of the substrate because only  $\{nn0\}$  planes satisfy Bragg diffraction conditions
14. H. Dal, E.W. Wong, Y.Z. Lu, S. Fan, C.M. Lieber, *Nature* **359**, 769 (1995); E.W. Wong, P.E. Sheehan, C.M. Lieber, *Science* **277**, 1971 (1997); J. Liu *et al.*, *Science* **280**, 1253 (1998); Q.W. Han, S.S. Fan, Q.G. Li, Y.D. Hu, *Science* **277**, 1287 (1997)
15. T.J. Trentler *et al.*, *Science* **270**, 1791 (1995)
16. K.P. Kumar, *Nature* **358**, 48 (1992)
17. According to  $\text{NaCl-Na}_2\text{O-TiO}_2$  phase diagram, no liquid phase appears below 800 °C (refer to phase diagram from ceramist, 1969 supplement, The American Ceramic Society, Inc., p. 473)
18. U. Gesenhues, *Solid State Ionics* **101-103**, 1171 (1997)
19. Y. Gao, K.L. Merkle, H.L. Chang, T.J. Zhang, D.J. Lam, *Phil. Mag. A* **65**, 1103 (1992)
20. G.L. Li, G.H. Wang, J.M. Hong, *J. Mater. Sci. Lett.* **18**, 1243 (1999)
21. H. Iwanaga, M. Egashira, K. Suzuki, M. Ichihara, S. Tacheuchi, *Philos. Mag. A* **58**, 683 (1988)
22. S. Smunnix, M. Schmeits, *Phys. Rev. B* **31**, 3369 (1985)
23. P. Jones, J.A. Hockey, *Trans. Faraday Soc.* **67**, 1679 (1971)